Second sound and the density response function in uniform superfluid atomic gases

H. Hu

ACQAO and Centre for Atom Optics and Ultrafast Spectroscopy, Swinburne University of Technology, Melbourne, Victoria 3122, Australia and Department of Physics, Renmin University of China, Beijing 100872, China

E. Taylor

Department of Physics, The Ohio State University, Columbus, Ohio, 43210, USA

X.-J. Liu

ACQAO and Centre for Atom Optics and Ultrafast Spectroscopy, Swinburne University of Technology, Melbourne, Victoria 3122, Australia

S. Stringari

CNR-INFM BEC Centre and Dipartimento di Fisica, Università di Trento, I-38050 Povo, Trento, Italy

A. Griffin

Department of Physics, University of Toronto, Toronto, Ontario, M5S 1A7, Canada

(Dated: Apr. 26, 2010)

Abstract

Recently there has been renewed interest in second sound in superfluid Bose and Fermi gases. By using two-fluid hydrodynamic theory, we review the density response $\chi_{nn}(\mathbf{q},\omega)$ of these systems as a tool to identify second sound in experiments based on density probes. Our work generalizes the well-known studies of the dynamic structure factor $S(\mathbf{q},\omega)$ in superfluid ^{4}He in the critical region. We show that, in the unitary limit of uniform superfluid Fermi gases, the relative weight of second vs. first sound in the compressibility sum rule is given by the Landau–Placzek ratio $\epsilon_{\rm LP} \equiv (\bar{c}_p - \bar{c}_v)/\bar{c}_v$ for all temperatures below T_c. In contrast to superfluid ^{4}He, $\epsilon_{\rm LP}$ is much larger in strongly interacting Fermi gases, being already of order unity for $T \sim 0.8T_c$, thereby providing promising opportunities to excite second sound with density probes. The relative weights of first and second sound are quite different in $S(\mathbf{q},\omega)$ (measured in pulse propagation studies) as compared to ${\rm Im}\chi_{nn}(\mathbf{q},\omega)$ (measured in two-photon Bragg scattering). We show that first and second sound in $S(\mathbf{q},\omega)$ in a strongly interacting Bose-condensed gas are similar to those in a Fermi gas at unitarity. However, in a weakly interacting Bose gas, first and second sound are mainly uncoupled oscillations of the thermal cloud and condensate, respectively, and second sound has most of the spectral weight in $S(\mathbf{q},\omega)$. We also discuss the behaviour of the superfluid and normal fluid velocity fields involved in first and second sound.

PACS numbers: 03.75.Kk, 03.75.Ss, 67.25.D-

I. INTRODUCTION

The most dramatic effects related to superfluidity in liquid ^{4}He arise [1] when the dynamics of the two components are described by the two-fluid hydrodynamics first discussed by Landau [2]. These equations only describe the dynamics when the non-equilibrium states are in local hydrodynamic equilibrium [3], which requires short collision times between the excitations forming the normal fluid. (This requirement is usually summarized as $\omega\tau \ll 1$, where ω is the frequency of a collective mode and τ is the appropriate relaxation rate.) The study of ultracold gases when they are in local equilibrium has been difficult because the density and the s-wave scattering length are typically not large enough. However, recent experimental work on trapped Bose-condensed gases has reported some success, with evidence for a second sound mode in highly elongated (cigar-shaped) traps [4].

Another approach to achieving conditions where the Landau two-fluid description is correct has been to consider a Fermi superfluid gas close to unitarity [5], where the s-wave scattering length between Fermi atoms in two different hyperfine states is infinite. Developing earlier theoretical studies [6, 7], Taylor and co-workers [8] have recently given detailed predictions for the first and second sound breathing oscillations in a trapped Fermi gas at unitarity. The coupled differential equations of the Landau two-fluid description were solved variationally, with results which agreed with analytic predictions at $T \to 0$ and $T \to T_c$. So far, only an isotropic trap has been studied.

In [8], it was shown that (as in superfluid ^{4}He) the frequencies of first and second sound in unitary Fermi gases were quite well approximated by assuming that the solutions of the two-fluid equations corresponded to pure uncoupled density and temperature waves. This is in sharp contrast to the situation in dilute, weakly interacting Bose gases, where first and second sound involve both density and temperature oscillations [9]. Naïvely, the first result above would lead one to believe that second sound in a unitary Fermi gas would have very small weight in the density response function. However, Arahata and Nikuni [10] have shown that in a uniform Fermi gas at unitarity, a density disturbance can have first and second sound pulses of comparable magnitude at temperatures of order $0.8T_c$.

The purpose of this paper is to provide a systematic study of the density response function $\chi_{nn}(\mathbf{q}, \omega)$ of a uniform superfluid atomic gas in the hydrodynamic regime [11, 12], as described by the non-dissipative Landau two-fluid equations (see sections II and III).

In this hydrodynamic region, the related dynamic structure factor is given by $S(\mathbf{q},\omega) \propto \mathrm{Im}\chi_{nn}(\mathbf{q},\omega)/\omega$. In studies of superfluid ^{4}He, $S(\mathbf{q},\omega)$ is directly measured in Brillouin light scattering experiments [13, 14]. In dilute gases, density pulse propagation experiments effectively measure $S(\mathbf{q},\omega)$ as noted in [10]. In addition, experiments using two-photon Bragg scattering have a cross-section proportional to $\mathrm{Im}\chi_{nn}(\mathbf{q},\omega)$. While all these experiments probe the same density response function, $\mathrm{Im}\chi_{nn}(\mathbf{q},\omega)$, the relative weight of the low frequency resonances are strongest in $S(\mathbf{q},\omega)$ because of the extra factor of $1/\omega$ noted above. This fact has significant implications for measuring second sound since the frequency of second sound becomes much smaller than first sound as T_c is approached.

We relate our analysis to classic discussions of the dynamic structure factor $S(\mathbf{q},\omega)$ in the two-fluid region of superfluid ^{4}He in the critical region [13–17]. However, many new features arise when dealing with quantum gases.

New aspects of our work include the use of the compressibility sum rule (sections III and IV) in understanding the relative weights of first and second sound in the density response function. We also discuss the role played by the Landau–Placzek ratio $\epsilon_{\mathrm{LP}} \equiv (\bar{c}_p - \bar{c}_v)/\bar{c}_v$ in determining these weights, with emphasis on new aspects that arise in superfluid gases. Here, $\bar{c}_p$ and $\bar{c}_v$ are the specific heats per unit mass at constant pressure and volume, respectively. We discuss the differences between $S(\mathbf{q},\omega)$ of a unitary Fermi gas and that of a Bose-condensed gas (sections IV and V), and present results for Bragg scattering with localized beams applied to the centre of a trapped unitary Fermi gas using the local density approximation (section VI). In B, we provide a detailed analysis of the superfluid and normal fluid velocity fields associated with first and second sound.

II. DENSITY RESPONSE FUNCTION

In this section, we review some basic properties of the density response function $\chi_{nn}(\mathbf{q},\omega)$, the related dynamic structure factor $S(\mathbf{q},\omega)$, and the experiments that measure these quantities. The density response function involves the correlation between the density at two different points at different times:

$$\chi_{nn}(\mathbf{r},t) \equiv -i\theta(t)\,\langle[\hat{\rho}(\mathbf{r},t),\hat{\rho}(\mathbf{0},0)]\rangle\,. \tag{1}$$

Here, $\theta(t)$ is the step function and we have set the volume equal to unity. The Fourier transform $\mathrm{Im}\chi_{nn}(\mathbf{q},\omega)$ of the imaginary part of the density response function is related to the dynamic structure factor $S(\mathbf{q},\omega)$ by

$$\begin{aligned} \mathrm{Im}\,\chi_{nn}(\mathbf{q},\omega+i0^+) &= -n\pi[S(\mathbf{q},\omega)-S(-\mathbf{q},-\omega)] \\ &= -n\pi\, S(\mathbf{q},\omega)(1-e^{-\beta\hbar\omega}), \end{aligned} \tag{2}$$

where n is the density, $\beta = 1/T$ is the inverse temperature, and in the last step we have made use of the "detailed balance" relation, $S(\mathbf{q},-\omega) = e^{-\beta\omega}S(\mathbf{q},\omega)$ and also the inversion symmetry of the system which gives $S(-\mathbf{q},\omega) = S(\mathbf{q},\omega)$. Here and throughout this paper we set $\hbar = k_B = 1$. Equation (2) can also be re-written as

$$S(\mathbf{q},\omega) = -\frac{1}{\pi n}[N^0(\omega)+1]\mathrm{Im}\,\chi_{nn}(\mathbf{q},\omega+i0^+), \tag{3}$$

where $N^0(\omega) = (e^{\beta\omega}-1)^{-1}$ is the Bose distribution function. The latter arises in both Bose and Fermi fluids because density fluctuations always obey Bose statistics. We see from (2) that $\mathrm{Im}\chi_{nn}(\mathbf{q},\omega)$ is the antisymmetric (frequency) part of the dynamic structure factor $S(\mathbf{q},\omega)$.

The dynamic structure factor $S(\mathbf{q},\omega)$ is measured by using inelastic scattering (e.g., neutron and Brillouin light scattering) of probe particles, which transfer momentum $\mathbf{q}$ and energy ω to the system. $S(\mathbf{q},\omega)$ is discussed and calculated in all standard texts on many body physics (convenient reviews are given in [18, 19]). In contrast, the density response function $\chi_{nn}(\mathbf{q},\omega)$ describes the density fluctuation induced by an external perturbing potential. As an example, in atomic gases, the imaginary part of the density response function is probed in two-photon Bragg scattering and also describes the density pulse produced by a blue-detuned laser. Brillouin and neutron scattering have been used extensively to study the collective modes in ^{4}He. These techniques cannot be applied to dilute atomic gases, however, since the gases are far too dilute to generate an appreciable signal. Instead, spectroscopic probes of dilute gases have successfully used Bragg scattering since this technique makes use of the stimulated light scattering processes induced by two counter-propagating laser beams, resulting in a strong enhancement of the signal.

In Bragg scattering experiments (see, e.g., [20]), by measuring the total momentum transferred to the sample, one measures the imaginary part of the density response function $\chi_{nn}(\mathbf{q},\omega)$, where $\mathbf{q}$ and ω are the momentum and energy transferred by the stimulated absorption and emission of the photons [18]. If the Bragg pulse is short compared to $2\pi/\omega_z$,

Method	System	Quantity measured	Response function
Bragg Spectroscopy	Gases	Momentum transferred	$\mathrm{Im}\chi_{nn}(\mathbf{q},\omega)$
Neutron Spectroscopy	^{4}He	Number of scattered neutrons	$S(\mathbf{q},\omega)$
Brillouin Spectroscopy ($\omega \ll T$)	^{4}He	Number of scattered photons	$S(\mathbf{q},\omega) \sim \frac{T}{\omega}\mathrm{Im}\chi_{nn}(\mathbf{q},\omega)$
Density pulse	Gases	Pulse amplitude	$\frac{1}{\omega}\mathrm{Im}\chi_{nn}(\mathbf{q},\omega)$

TABLE I: Summary of experimental probes. From left to right: the experimental method, the system(s) to which the method can be applied, the quantity being measured, and the density response function involved. In the two-fluid region of strongly interacting Fermi gases and ^{4}He, second sound is weakly coupled to density fluctuations but has a small frequency ω at high temperatures (below T_c). This means that, as a result of the extra factor of $1/\omega$ multiplying the density response function, Brillouin spectroscopy and density pulses are more sensitive to second sound than Bragg and neutron scattering.

where ω_z is the frequency of the harmonic trap along the axis of light propagation ($\mathbf{q} = \hat{\mathbf{z}}q$), the momentum transferred is

$$\Delta P_z = 2q\tau \left(\frac{V}{2}\right)^2 \mathrm{Im}\chi_{nn}(q,\omega), \tag{4}$$

where V is the strength of the potential induced by the lasers and τ is the pulse duration.

As noted recently by Arahata and Nikuni [10], the density response function can also be measured by exciting a density pulse in a uniform gas. Within linear response theory, the density fluctuation $\delta n(\mathbf{r},t)$ induced by the application of an external perturbing potential $\delta V(\mathbf{r},t)$ is

$$\delta n(\mathbf{r},t) = \int \frac{d\mathbf{q}}{(2\pi)^3} \int \frac{d\omega}{2\pi} \chi_{nn}(\mathbf{q},\omega)\delta V(\mathbf{q},\omega) e^{i\mathbf{q}\cdot\mathbf{r}-i\omega t}, \tag{5}$$

where $\delta V(\mathbf{q},\omega)$ is the Fourier transform of the perturbing potential. Similar to the sound propagation experiments in [21, 22], consider a localized potential applied for a short duration $\tau < t < 0$, and turned off at $t = 0$. Assuming for simplicity that the perturbing

potential only varies spatially along the z-axis (and $\mathbf{q} = \hat{\mathbf{z}}q$), for $t > 0$, one obtains [10]

$$\delta n(z,t) = \frac{1}{2\pi^2}\int dq \int d\omega \delta V(q) \frac{\mathrm{Im}\chi_{nn}(q,\omega)}{\omega} e^{iqz - i\omega t}. \tag{6}$$

Equation (6) reveals an important feature: in contrast to Bragg scattering, where the response is proportional to $\mathrm{Im}\chi_{nn}(\mathbf{q},\omega)$, the response involved in the excitation of density pulses in proportional to $\mathrm{Im}\chi_{nn}(\mathbf{q},\omega)/\omega$. As we discuss in section III, for uniform superfluids, this factor of $1/\omega$ leads to an enhancement in the signal of second sound in density pulse experiments as compared to its signal in Bragg spectroscopy. In table I, we review the quantities measured by the experimental probes of interest in both dilute gases and superfluid ^{4}He.

Before discussing the form of the density response function in the two-fluid hydrodynamic region in section III, we first review below some general properties of the dynamic structure factor that will be of use later on in understanding the contributions from first and second sound in experimental probes of superfluid atomic gases.

Quite generally, $S(\mathbf{q},\omega)$ satisfies various frequency moment sum rules. Two are of special particular interest in the two-fluid domain [23]. The f-sum rule (valid for all q) is

$$\int_{-\infty}^{\infty} \omega\, S(\mathbf{q},\omega) = \frac{q^2}{2m}. \tag{7}$$

The compressibility sum rule arises from the exact Kramers-Kronig identity (also valid for all q)

$$\chi_{nn}(\mathbf{q},\omega=0) = \int_{-\infty}^{\infty} \frac{d\omega'}{\pi} \frac{\mathrm{Im}\chi_{nn}(\mathbf{q},\omega')}{\omega'}, \tag{8}$$

which involves an inverse frequency moment. (Note that $\chi_{nn}(\mathbf{q},\omega=0) = \mathrm{Re}\chi_{nn}(\mathbf{q},\omega=0)$ is purely real.) Using (2), one can show that (8) is equivalent to

$$\chi_{nn}(\mathbf{q},\omega=0) = -2n\int_{-\infty}^{\infty} d\omega' \frac{S(\mathbf{q},\omega')}{\omega'}. \tag{9}$$

The usefulness of (8) and (9) is due to the fact that in the long wavelength limit ($\mathbf{q} \to 0$), the density response function $\chi_{nn}(\mathbf{q}=0,\omega=0)$ describes static thermodynamic fluctuations which can be related to the equilibrium isothermal compressibility [23, 24]

$$\lim_{q\to 0} \chi_{nn}(\mathbf{q},\omega=0) = -n \left.\frac{\partial n}{\partial p}\right|_T. \tag{10}$$

Thus we arrive at the so-called compressibility sum rule for the dynamic structure factor,

$$\lim_{q\to 0} \int_{-\infty}^{\infty} d\omega' \frac{S(\mathbf{q},\omega')}{\omega'} = \frac{1}{2m}\left.\frac{\partial \rho}{\partial p}\right|_T \equiv \frac{1}{2mv_T^2}, \tag{11}$$

where we have introduced the isothermal sound velocity v_T.

The sum rules in (7) and (11) are general and may be viewed as two constraints which $S(\mathbf{q},\omega)$ must always satisfy. The $f-$sum rule is used frequently in discussions of inelastic neutron scattering as a check on the experimental data. As we discuss in section III, the compressibility sum rule has special significance when we discuss the two-fluid hydrodynamic region, as first emphasized by Nozières and Pines [23].

III. DYNAMIC STRUCTURE FACTOR IN THE TWO-FLUID REGIME

The Landau two-fluid equations for an isotropic (such that $\chi_{nn}(\mathbf{q},\omega) = \chi_{nn}(q,\omega)$) superfluid (Bose or Fermi) describe the dynamics when collisions are strong enough to produce local equilibrium. Using the non-dissipative two-fluid equations, one finds the density response function (see Refs. [11, 12] and page 138 of [3]),

$$\chi_{nn}(q,\omega) = \frac{nq^2}{m}\frac{\omega^2 - v^2q^2}{(\omega^2 - u_1^2q^2)(\omega^2 - u_2^2q^2)}, \tag{12}$$

where we have defined a new velocity

$$v^2 \equiv T\frac{\bar{s}_0^2}{\bar{c}_v}\frac{\rho_{s0}}{\rho_{n0}}. \tag{13}$$

Here, $\bar{s}_0 \equiv S_0/Nm$ is the equilibrium entropy S_0 per unit mass and $\bar{c}_v \equiv T(\partial\bar{s}/\partial T)_\rho$ is the specific heat per unit mass at constant volume. The equilibrium superfluid and normal fluid densities are denoted by ρ_{s0} and ρ_{n0}, respectively. In (12), u_1 and u_2 are the well-known exact first and second sound velocities given by Landau's hydrodynamics. For later purposes, we note that these velocities satisfy the exact relations

$$u_1^2 + u_2^2 = v^2 + v_{\bar{s}}^2, \quad u_1^2u_2^2 = v_T^2v^2 = v_{\bar{s}}^2\frac{v^2}{\gamma}, \tag{14}$$

where v_T is defined in (11) and the adiabatic sound velocity is defined as

$$v_{\bar{s}}^2 \equiv \left.\frac{\partial P}{\partial\rho}\right|_{\bar{s}}. \tag{15}$$

We note that thermodynamic relations [24] show that, quite generally, the ratio of the specific heats can be related to the isothermal and adiabatic sound velocities,

$$\gamma \equiv \frac{\bar{c}_p}{\bar{c}_v} = \frac{v_{\bar{s}}^2}{v_T^2}. \tag{16}$$

The difference between $v_{\bar{s}}$ and v_T is a consequence of the finite thermal expansion.

Equation (12) gives the density response for Bose and Fermi fluids described by the non-dissipative Landau two-fluid equations. The two-fluid density response function in the presence of dissipation arising from transport coefficients has been given by Hohenberg and Martin [11, 12, 15]. (See also the discussion given by Vinen [14].) For our purposes in this paper, the primary effect of dissipation is to broaden the delta function peaks in the imaginary part of the non-dissipative density response function. It does not otherwise change the structure of the two-fluid response function and in particular, does not affect in a significant way the weights of first and second sound in this function.

From (12), it is straightforward to obtain the imaginary part of the density response function, which is the experimentally relevant quantity in dilute gases:

$$\begin{aligned} \mathrm{Im}\chi_{nn}(q,\omega) \;=\; -n\pi\frac{q^2}{2m}\Big\{&\frac{Z_1}{\omega}\left[\delta(\omega-u_1q)+\delta(\omega+u_1q)\right] \\ &+\frac{Z_2}{\omega}\left[\delta(\omega-u_2q)+\delta(\omega+u_2q)\right]\Big\}. \end{aligned} \tag{17}$$

Here, we have defined the "traditional" amplitudes for first and second sound, namely

$$Z_1 \equiv \frac{u_1^2-v^2}{u_1^2-u_2^2}\;,\;\; Z_2 \equiv \frac{v^2-u_2^2}{u_1^2-u_2^2}. \tag{18}$$

Using (17) in (3), the two-fluid expression for the dynamic structure factor is found to be

$$\begin{aligned} S(q,\omega) = \frac{q^2}{2m}[N^0(\omega)+1]\Big\{&\frac{Z_1}{\omega}\left[\delta(\omega-u_1q)+\delta(\omega+u_1q)\right] \\ &+\frac{Z_2}{\omega}\left[\delta(\omega-u_2q)+\delta(\omega+u_2q)\right]\Big\}. \end{aligned} \tag{19}$$

The two-fluid dynamic structure factor in (19) turns out to satisfy both the f-sum and compressibility sum rules, given by (7) and (11) [23]. This makes use of the identity $N^0(\omega)+1+N^0(-\omega)+1=1$, satisfied by the Bose distribution. Substituting (19) into the left-hand side of (7), one sees that the amplitudes Z_1 and Z_2 describe the weights of first and second sound, respectively, in the f-sum rule. That the sum of these two contributions saturate the f-sum rule is a consequence of the fact that $Z_1+Z_2=1$. Similarly, substituting (19) into the left-hand side of (11), one sees the relative contributions of first and second sound to the isothermal compressibility are given by Z_1/u_1^2 and Z_2/u_2^2, respectively. We will denote these weights by W_i:

$$W_1 \equiv \frac{Z_1}{u_1^2},\;\; W_2 \equiv \frac{Z_2}{u_2^2}. \tag{20}$$

To see that the compressibility sum rule is saturated by these contributions from first and second sound, we note that $Z_1/u_1^2 + Z_2/u_2^2 = 1/v_T^2$, as can be seen from (14).

Since we are working in the low frequency two-fluid hydrodynamic region, we can use the fact that $\omega \ll T$. In this limit, the detailed balance factor in (19) can be approximated by

$$N^0(\omega) + 1 \simeq \frac{T}{\omega} + \frac{1}{2} + \dots \tag{21}$$

The first quantum correction, given by the 1/2 term in (21) in this expansion, is needed to satisfy the sum rules previously discussed. This approximation ($\omega \ll T$) is often referred to as the "classical limit" in textbooks discussing the dynamic structure factor, although in fact it describes both superfluid ($T < T_c$) and normal fluid ($T > T_c$) collisional hydrodynamics.

Keeping only the leading order first term in (21), (19) simplifies to

$$\begin{aligned} S(q,\omega) \;&\simeq\; \frac{T}{2m}\Bigg\{ \frac{Z_1}{u_1^2}\left[\delta(\omega - u_1 q) + \delta(\omega + u_1 q)\right] \\ &\qquad + \frac{Z_2}{u_2^2}\left[\delta(\omega - u_2 q) + \delta(\omega + u_2 q)\right] \Bigg\} \\ &=\; -\frac{1}{\pi n}\left(\frac{T}{\omega}\right) \mathrm{Im}\chi_{nn}(q,\omega). \end{aligned} \tag{22}$$

This expression is valid for Bose and Fermi superfluid gases as well as superfluid ^{4}He, that is, all superfluids described by an order parameter with a phase and amplitude. Equation (22) shows that in the low-frequency two-fluid hydrodynamic region, $W_i \equiv Z_i/u_i^2$ gives the weight of the i^{th} mode. In contrast, the weight of the i^{th} mode in Bragg scattering [see (4) and (17)] is given by B_i, where

$$B_1 \equiv \frac{Z_1}{u_1}, \quad B_2 \equiv \frac{Z_2}{u_2}. \tag{23}$$

Comparing (22) with (17), we see that the hydrodynamic limit ($\omega \ll T$) of $S(q,\omega)$ involves an extra factor of $1/\omega$.

We see that while $\mathrm{Im}\chi_{nn}(q,\omega)$ and $\mathrm{Im}\chi_{nn}(q,\omega)/\omega$ share the same poles, the relative weights of first and second sound are quite different in these two functions, with $B_2/B_1 = (W_2/W_1)(u_2/u_1)$ generally being much smaller than W_2/W_1 due to the smallness of u_2/u_1 (see Fig. 1).

The two-fluid expression in (22) is known from earlier discussions of Brillouin scattering in superfluid ^{4}He (see section IV). In contrast to high-frequency inelastic neutron scattering, Brillouin scattering is carried out with light in the visible part of the spectrum ($\omega \ll T$). As pointed out above [see (22)], this means that Brillouin scattering measures the imaginary

part of the density response function divided by the frequency ω. In studies of superfluid ^{4}He, this factor of $1/\omega$ is crucial to probing second sound since, although only weakly coupled to density, the speed of second sound is small and hence, its weight in Brillouin light scattering can be significant.

As noted in section II, a similar situation arises in studies of pulse propagation in dilute gases, albeit for very different reasons. In this situation [see (6)], the amplitude of the density pulse induced by a localized (in time and space) density perturbation is proportional to $\mathrm{Im}\chi_{nn}(q,\omega)/\omega$. The factor of $1/\omega$ here results not from the detailed balance factor, but from the Fourier transform of the step-function used to model the time dependence of the perturbing laser beams. Arahata and Nikuni [10] calculated the effect of producing a density fluctuation by a sudden perturbation in a superfluid Fermi gas at unitarity. The final result was two pulses moving with the speeds of first and second sound, with relative amplitudes given by W_i as defined in (20).

IV. SUPERFLUIDS WITH SMALL THERMAL EXPANSION

In section III, we showed that the relative weights in $S(q,\omega)$ and $\mathrm{Im}\chi_{nn}(q,\omega)$ of first and second sound are given by $W_i = Z_i/u_i^2$ and $B_i = Z_i/u_i$, respectively, where Z_i is defined in (18). These results are valid for any type of superfluid, including weakly interacting atomic Bose gases and also strongly interacting Fermi gases. In this section, we concentrate on strongly interacting Fermi gases where, as discussed above, the thermal expansion is relatively small, meaning that density and temperature fluctuations are not strongly coupled. Using the exact relations in (14), in this section we will show that to a very good approximation, W_2/W_1 is given by (30) in this situation. In section V, we give a brief discussion of the dynamic structure factor in a dilute Bose gas, where the thermal expansion can be much larger when the s-wave scattering length is small.

Solving the coupled equations in (14), one obtains the expansions [14, 15]

$$u_1^2 = v_s^2[1 + (\gamma - 1)x + \cdots], \quad u_2^2 = \frac{v^2}{\gamma}[1 - (\gamma - 1)x + \cdots], \tag{24}$$

in terms of the parameter defined by $x \equiv v^2/\gamma v_s^2$. These results show that to lowest order in the parameter $x(\gamma - 1) \equiv x\epsilon_{\mathrm{LP}}$, the first and second sound velocities are well approximated

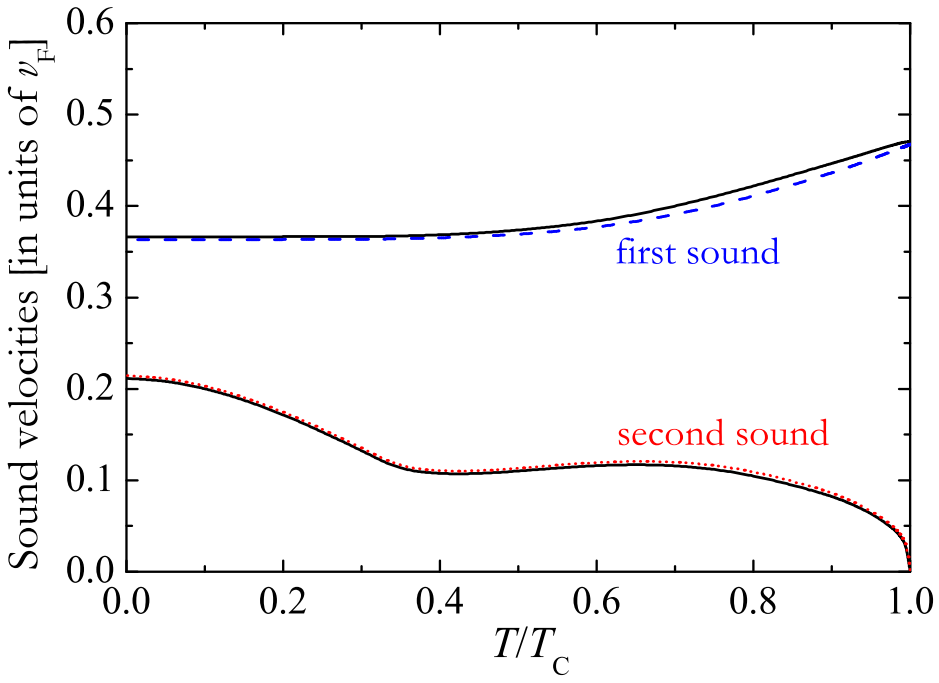

FIG. 1: Speeds of first and second sound in a unitary superfluid Fermi gas. The dashed lines are the approximations $c_1 = v_{\bar{s}}$ and $c_2 = v/\sqrt{\gamma}$, as given by the leading terms in (24) (from [8]).

by

$$c_1^2 = v_{\bar{s}}^2, \quad c_2^2 = \frac{v^2}{\gamma} = T\frac{\bar{s}_0^2}{\bar{c}_p}\frac{\rho_{s0}}{\rho_{n0}}. \tag{25}$$

In figure 1, we show the temperature dependence of u_1 and u_2 and compare these results with the leading order expressions c_1 and c_2 given by (25) (shown by the dashed lines). The thermodynamic functions needed to obtain these sound speeds are calculated using the microscopic theory of Nozières and Schmitt-Rink (NSR) [25, 26]. We see that c_1 and c_2 are extremely good approximations at all temperatures. At temperatures $T \gtrsim 0.4T_c$, $x = c_2^2/c_1^2$ is very small, even though $\epsilon_{\rm LP} \sim \mathcal{O}(1)$. At lower temperatures, while x is no longer small ($x = 1/3$ at $T = 0$), $\epsilon_{\rm LP}$ becomes extremely small. Thus in both limits, we find that the correction term $x\epsilon_{\rm LP}$ in (24) is negligible.

The fact that $u_1 \simeq c_1$ and $u_2 \simeq c_2$ in a fluid with small thermal expansion such as the unitary Fermi gas means that first and second sound propagate at essentially the same velocities as pure density and temperature oscillations, as would arise when $\epsilon_{\rm LP} = 0$. Surprisingly, this does not mean that first and second sound are uncoupled density and temperature oscillations. We discuss this in detail in B.

Two-fluid hydrodynamics leads to the coupled equations [2, 3]

$$u^2\delta\rho = \delta P, \;\; u^2\delta\bar{s} = \bar{s}_0^2\frac{\rho_{s0}}{\rho_{n0}}\delta T. \tag{26}$$

As noted above (see figure 1), the speeds of first and second sound are well approximated by c_1 and c_2 in (25). Physically, this means that to leading order, the pressure fluctuations in first sound are at constant entropy per unit mass $\bar{s}$ and hence, $\delta P \simeq (\partial P/\partial\rho)_{\bar{s}}\delta\rho$. Similarly, the temperature fluctuations in second sound are to leading order at constant pressure and hence, $\delta T \simeq (\partial T/\partial\bar{s})_p\delta\bar{s}$. Using these in (26) leads to the leading order expressions for u_1 and u_2 given in (24).

We remark that, qualitatively, our results in figure 1 for the temperature dependence of u_1 and u_2 are in agreement with Arahata and Nikuni [10], who also based their work on NSR thermodynamics. The differences with [10] at high and low temperatures are easily understood. Direct numerical calculations based on NSR are difficult to do accurately for $T < 0.4T_c$ because of the extremely small value of the normal fluid density. Our results in figure 1 in this region are based on the assumption that Goldstone phonons are the dominant thermal excitations at low T at unitarity, which allows us to obtain the low temperature values of u_1 and u_2 analytically. In the opposite limit of high temperatures close to T_c, our calculations show that W_2 steadily increases, in contrast with that of [10]. For T close to T_c, it is crucial to use a superfluid density with the correct critical behaviour [27], removing the spurious first-order behaviour predicted by NSR [28]. (In fact, this behaviour is not unique to NSR and is symptomatic of any theory that treats phase fluctuations in a perturbative way. See [29] for further discussion.)

Using the values of u_1, u_2, and v (see figure 1), we can calculate Z_2, W_2 and W_1. The results are shown in figure 2. The relative weight of second and first sound in $S(q,\omega)$ is given by

$$\frac{W_2}{W_1} = \frac{Z_2u_1^2}{Z_1u_2^2} = \frac{v^2-u_2^2}{u_1^2-v^2}\frac{u_1^2}{u_2^2}. \tag{27}$$

Using the exact two-fluid expressions for u_1 and u_2 gives the ratio W_2/W_1 shown in figure 3. For comparison, we also plot the Landau-Placzek ratio $\epsilon_{\rm LP} = \gamma - 1$, calculated directly from the same thermodynamic functions used to obtain the sound speeds u_1, u_2, and v [7, 8].

In figure 4, we plot $S(q,\omega)$ given by (22). This shows the first and second sound resonances at a series of temperatures. The results shown in figures 2-4 show the remarkable feature that, even though the maximum value of Z_2 is ~ 0.05 at $T \sim 0.8T_c$, the relative weights of

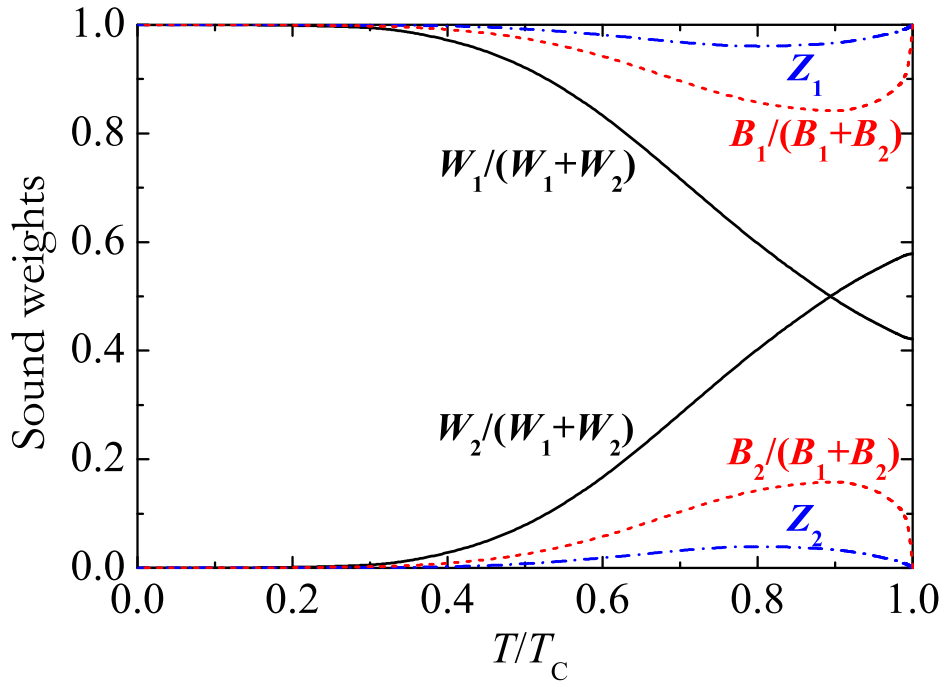

FIG. 2: The temperature dependence of the normalized amplitudes Z_i, B_i, and W_i of first ($i = 1$) and second sound ($i = 2$) in a Fermi gas at unitarity.

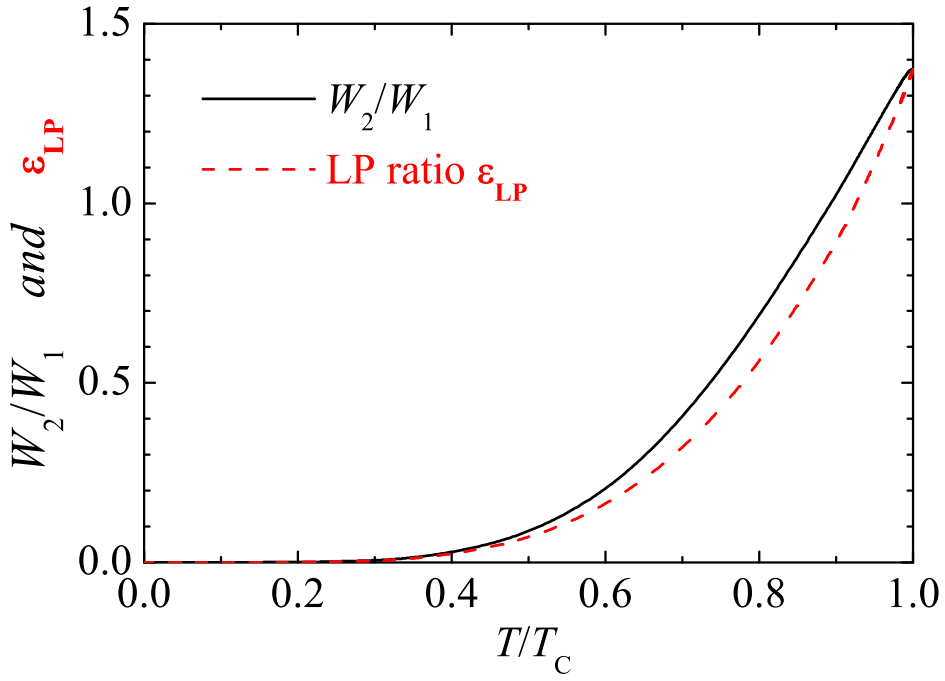

FIG. 3: Comparison between the ratio of the second and first sound amplitudes (W_2/W_1) and the Landau-Placzek ratio $\epsilon_{\rm LP} = \gamma - 1$ in a unitary Fermi gas.

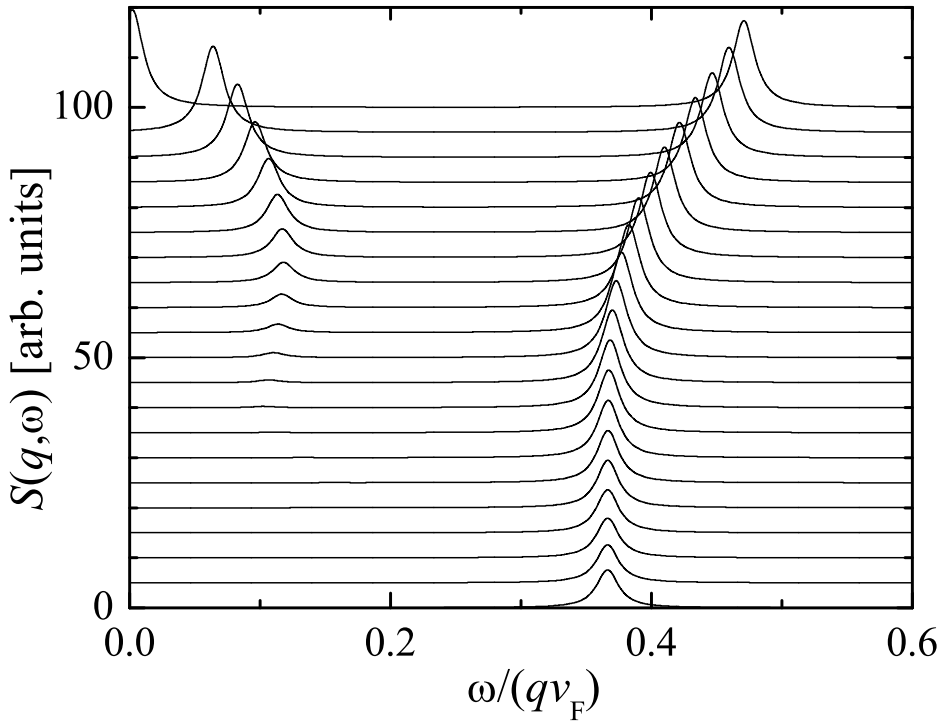

FIG. 4: The two-fluid dynamic structure factor given by (22) at unitarity. The plot shows the first and second sound resonances as a function of the frequency ω/qv_F (where we take $q = 0.1k_F$ and v_F is the Fermi velocity) for a series of temperatures from $T = 0$ to $T = T_c$, in steps of $0.05T_c$ (each temperature is offset). For clarity, the delta functions in (22) are plotted as Lorentzians with a width $\Delta = 0.01qv_F$.

first and second sound in $S(q, \omega)$ can be comparable in the temperature region $T \gtrsim 0.8T_c$. The relative weight of second sound is instead much smaller in $\mathrm{Im}\chi_{nn}$ (see figure 5) for reasons we have discussed.

Figure 3 also shows that W_2/W_1 is quite well approximated by ϵ_{LP}. It is useful to derive this result more analytically. Using (14) in (27), we obtain after some algebra

$$\frac{W_2}{W_1} = \frac{1}{\epsilon_{\mathrm{LP}}} \left(\frac{u_1^2}{v_T^2} - 1 \right)^2 . \tag{28}$$

This expression was first given by Vinen [30]. Using the expansion for u_1^2 in (24), one can reduce (28) to

$$\frac{W_2}{W_1} = \epsilon_{\mathrm{LP}} (1 + \gamma x + \cdots)^2 . \tag{29}$$

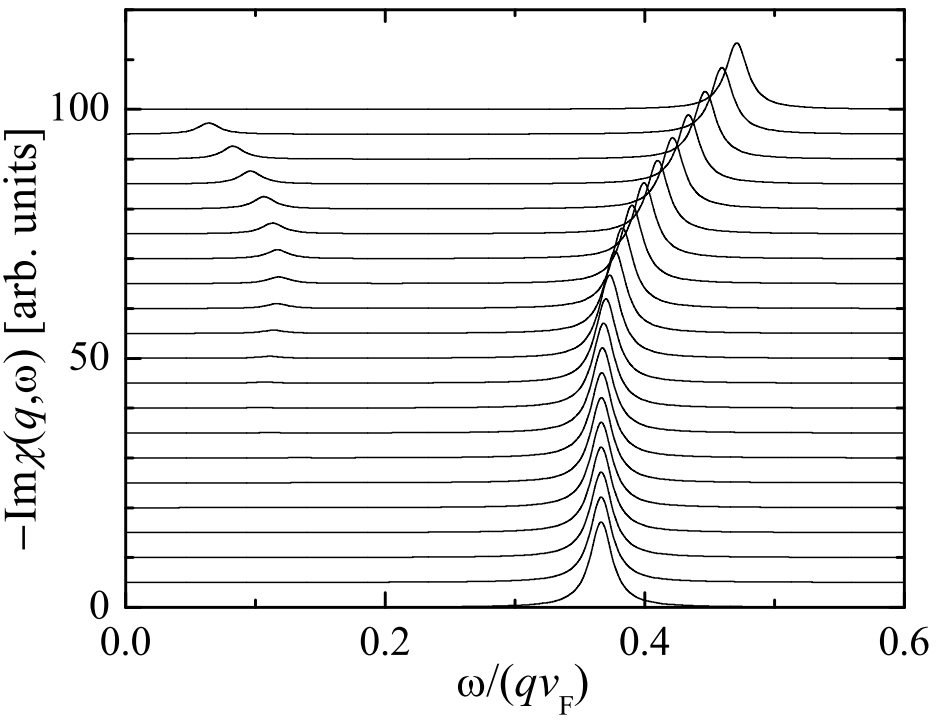

FIG. 5: The imaginary part of the two-fluid density response function at unitarity. In contrast to the results shown in figure 4, where the relative weights of second and first sound are determined by W_2/W_1, in Bragg scattering they are determined by the smaller ratio B_2/B_1 [see (23)]. As a result, second sound has a much smaller weight in Bragg scattering that first sound.

At high temperatures, where $x = c_2^2/c_1^2 \ll 1$ (see figure 1), we have

$$\frac{W_2}{W_1} = \epsilon_{\rm LP}[1 + 2(1+\epsilon_{\rm LP})x + \cdots] \simeq \epsilon_{\rm LP} = \gamma - 1. \tag{30}$$

This result was first obtained almost 40 years ago [11, 14, 15, 31] in the context of Brillouin light scattering [13] in superfluid ^{4}He near the critical region close to T_c. For $T \lesssim 0.4T_c$, one can see from figure 1 that we can no longer assume $x \ll 1$ and hence expand (29).

As noted above, the result in (30) was obtained in the classic literature on superfluid ^{4}He. The Landau-Placzek ratio $\epsilon_{\rm LP}$ is extremely small $(10^{-2} - 10^{-3})$ in superfluid ^{4}He and thus second sound has generally a very small amplitude in the dynamic structure factor. However, under pressure and close to T_c, the magnitude of $\epsilon_{\rm LP}$ in liquid ^{4}He can be significantly increased (to about $\epsilon_{\rm LP} \sim 0.2$) such that a second sound doublet in $S(q,\omega)$ can be measured using Brillouin light scattering techniques [13]. Such studies [16, 17] have verified the correctness of $W_2/W_1 = \epsilon_{\rm LP}$ in liquid ^{4}He at a pressure of $P = 25$ atmospheres in the

temperature region $(T_c - T) \sim 10^{-2} - 10^{-4} K$.

The Landau-Placzek ratio $\epsilon_{\rm LP} \equiv \gamma - 1$ was first derived in 1934 [32] to describe the relative weight of the thermal diffusion central peak vs. sound waves which are exhibited by $S(q, \omega)$ describing the hydrodynamics of a normal fluid. Thus, (30) generalizes the Landau-Placzek result [24, 32] to the case of two-fluid hydrodynamics. In a normal liquid above T_c, the dynamic structure factor given by (22) reduces to [24]

$$S(q, \omega) = \frac{T}{2m} \left\{ \frac{1}{v_{\bar{s}}^2} \left[\delta(\omega - v_{\bar{s}} q) + \delta(\omega + v_{\bar{s}} q) \right] + \frac{\gamma - 1}{v_{\bar{s}}^2} \delta(\omega) \right\}. \tag{31}$$

Thus, above T_c, the second sound doublet in (22) collapses into a zero frequency central peak, with relative weight $\gamma - 1$ compared to a sound wave at $\omega = v_{\bar{s}} q$. When one includes damping due to transport processes, the central peak in (31) broadens, describing the thermal diffusion relaxation mode of width $D_T q^2$ (where D_T is the thermal diffusivity). The behaviour of $S(q, \omega)$ as one goes from below T_c to above T_c is smooth but complicated due to various singularities in the thermodynamic and transport coefficients (for further discussion, see [14].)

V. DYNAMIC STRUCTURE FACTOR OF DILUTE BOSE GASES

In this section, we discuss first and second sound in a uniform dilute Bose-condensed gas. The two-fluid hydrodynamics is again described by the results given in section III. However, we need to distinguish between the cases of weakly and strongly interacting Bose gases. The latter case can be easily realized by considering a molecular Bose condensate on the BEC side of the BCS-BEC crossover in a two-component Fermi gas. In such a molecular Bose gas with density $n_B = n/2$ and molecular mass $m_B = 2m$, the s-wave molecular scattering length is given by $a_B \simeq 0.6 a_F$, where a_F is the atomic s-wave scattering length between the two Fermi components [33]. We will show that the behaviour of first and second sound in strongly interacting Bose gases is very similar to that in Fermi gas superfluids near unitarity, but very different from that in weakly interacting Bose gases.

In a dilute, weakly interacting Bose gas, the thermodynamic quantities that enter the two-fluid equations can be solved analytically in powers of the interaction strength $g \equiv 4\pi a_B / m_B$. To first order in g, the speeds of first and second sound are given by (see, for instance,

chapter 15 in [3])

$$u_1^2 = \frac{5T}{3m_B}\frac{g_{5/2}(1)}{g_{3/2}(1)} + \frac{2g\tilde{n}_0}{m_B}, \quad u_2^2 = \frac{gn_{c0}}{m_B}. \tag{32}$$

Here, $g_n(z) = \sum_{l=1}^{\infty} z^l/l^n$ is the usual Bose-Einstein function with fugacity z. In the limit of small g, the normal fluid density ρ_{n0} reduces to the density $m\tilde{n}_0 \equiv \rho - mn_{c0}$ of atoms thermally excited out of the condensate. The superfluid density ρ_{s0} is likewise given by the density mn_{c0} of condensate atoms. To lowest order in g, n_{c0} is the condensate density of the ideal Bose gas.

In figure 6, we show the temperature dependence of u_1 and u_2, satisfying (14), in the case of weak interactions ($n_B a_B^3 = 10^{-5}$). The thermodynamic functions used to determine these sound velocities have been calculated using the Hartree–Fock–Popov (HFP) microscopic model for the thermal excitations [3]. The velocities are normalized in terms of a Fermi velocity defined by $v_F = (6\pi^2 n_B)^{1/3}/m$ (equivalent to the Fermi velocity of a two component Fermi gas through the BCS-BEC crossover). We also show for comparison the values of u_1 and u_2 given by the lowest order solutions described by (32). One sees that these uncoupled modes of oscillations are a good first approximation to the full solutions of the two-fluid equations in a weakly interacting BEC at all temperatures outside a small temperature region at low temperatures where first and second sound hybridize, exhibiting an avoided crossing. At this avoided crossing, the natures of first and second sound are interchanged. As $T \to 0$, the first sound velocity coincides with the phonon velocity, as is the case with strongly interacting Fermi gases and superfluid ^{4}He. For a dilute gas, this phonon velocity is the Bogoliubov–Popov phonon velocity $\sqrt{gn_{c0}/m_B}$, and corresponds to an oscillation of the condensate component. Above the hybridization point, to a good approximation, second sound propagates with this velocity. Consequently, second sound in a dilute Bose gas (above the hybridization temperature) is essentially an oscillation of the condensate at all temperatures, with a static thermal cloud. In contrast, first sound describes an oscillation of the thermal cloud in the presence of a stationary condensate.

We note that HFP approximation we have used to calculate thermodynamic quantities has the well-known problem near T_c of predicting a spurious first-order transition (see, for instance, [34]). As touched on in section IV, this is actually a very general problem, and arises in any theory that treats bosonic phase fluctuations of the order parameter as a small parameter, including the HFP and NSR theories. Of course, this includes all perturbation

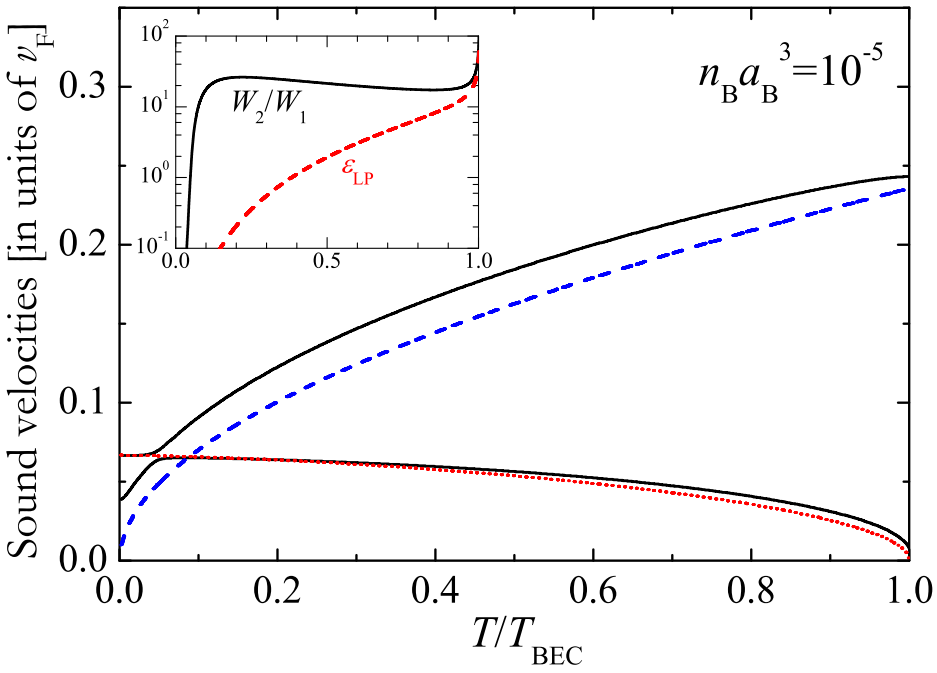

FIG. 6: Speeds of first and second sound in a weakly interacting molecular Bose gas with gas parameter $n_B a_B^3 = 10^{-5}$. The blue dashed and red dotted lines are respectively the approximate speeds u_1 and u_2 given by (32). The inset shows the LP ratio $\epsilon_{\rm LP}$ (red dashed line) and the weight ratio W_2/W_1 (black solid line).

theories that go beyond mean-field and only *ab initio* Quantum Monte-Carlo calculations can avoid this problem. (A competing fluctuation theory of the BCS-BEC crossover [35] avoids this problem by ignoring phase fluctuations.) The unphysical first-order transition leads to the result that the second sound velocity does not vanish at T_c as it should. In contrast to figure 1, we have not corrected the spurious behaviour of the superfluid (condensate) density close to T_c in the results shown in figures 6 and 7. These figures also show the expected feature that the error becomes larger with increasing interaction strength. In spite of the shortcomings of HFP theory in the critical region close to T_c, we emphasize that it gives a good estimate of thermodynamic quantities, outside the critical region. All numerical results shown in figures (6)-(8) are obtained using this theory (apart from the uncoupled solutions shown in figure 6, which use the ideal gas expression for the condensate density).

In figure 6, the inset shows the much larger value of the LP ratio $\epsilon_{\rm LP}$ (compared to a Fermi superfluid–see figure 3) and the ratio W_2/W_1 of the amplitudes of second and first

sound in $S(q,\omega)$ as a function of the temperature. We note that ratio W_2/W_1 is still given by the expressions in (27) and (28). However, now the parameter $\epsilon_{\rm LP}$ is no longer small ($\ll 1$) and thus the expansion based on (24), which leads to (29) and (30), is no longer valid. We also explicitly note that W_2/W_1 is not equal to $\epsilon_{\rm LP}$ in either the weak or strong coupling limits.

First and second sound in a dilute, weakly interacting Bose gas involve weakly coupled oscillations of the thermal cloud and condensate, respectively. Both modes contribute to the density response function. Consequently, both first and second sound are sensitive to density probes. This fact has been made use of in a recent experiment involving trapped atomic Bose gases by Meppelink *et al.* [4]. In this study, a density pulse was generated (as described in section II) and the velocity of the second sound pulse was measured above the hybridization point by tracking the propagation of the density pulse. The inset in figure 6 shows that the amplitude of second sound in $S(q,\omega)$ and in density pulse propagation experiments is twenty times as strong as first sound for all temperatures above the crossing point at $T \sim 0.1T_c$. This result may explain the absence of a first sound pulse in the data of [4], which corresponded to $n_B a_B^3 \sim 5 \times 10^{-6}$.

In figure 7, we plot first and second sound for a more strongly interacting Bose gas (i.e., with a larger value of g.) This situation is close to the unitarity Fermi gas results shown in figure 1 [36]. In particular, we see that the velocities of first and second sound never become degenerate (cross) and thus the hybridization shown in figure 6 does not occur. In this strongly interacting Bose superfluid, we also show the approximate velocities of u_1 and u_2 given by (25). These approximate values give a reasonable first order approximation to the full solutions of the first and second sound velocities, rather than the expression in (32) that applies to a weakly interacting Bose gas as shown in figure 6. The inset shows the ratio of W_2/W_1 vs. T, as computed from (27). In this case, the amplitude of second sound in $S\left(q,\omega\right)$ is only 2-3 times larger than first sound for $T \gtrsim 0.5T_c$.

In figure 8, we compare the values of $W_1/(W_1+W_2)$ and $W_2/(W_1+W_2)$ for a weakly interacting Bose gas ($n_B a_B^3 = 10^{-4}$) and a strongly interacting Bose gas ($n_B a_B^3 = 0.1$). One sees that the latter case is qualitatively similar to the result in a Fermi superfluid gas at unitarity given in figure 2. In contrast, in a weakly interacting Bose gas, for the temperature range above the hybridization point, the amplitude of second sound is much larger than first sound in both $S(q,\omega)$ and density pulse propagation experiments.

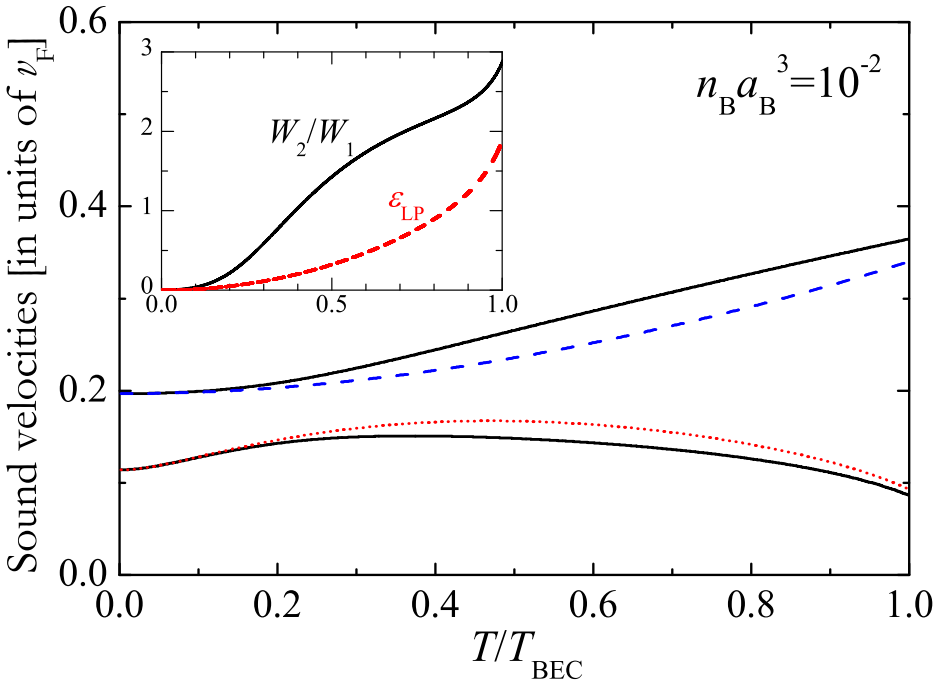

FIG. 7: Speeds of first and second sound in a strongly interacting molecular Bose gas with gas parameter $n_B a_B^3 = 10^{-2}$. The blue dashed and red dotted lines are respectively the approximate speeds $c_1 = v_{\bar{s}}$ and $c_2 = v/\sqrt{\gamma}$ given by (25). The inset shows the LP ratio $\epsilon_{\rm LP}$ (dashed line) and the weight ratio W_2/W_1 (black line), to be compared with the result in figure 3 for a strongly interacting Fermi gas at unitarity.

VI. BRAGG SCATTERING IN A TRAPPED ATOMIC GAS

For illustration, we now consider the response of a trapped Fermi gas at unitarity to two-photon Bragg scattering due to first and second sound. We consider an experimental setup similar to that used in [37], where a pair of laser beams are applied to the gas such that the region where they overlap is confined to the centre of the gas. As a first approximation to this configuration, we assume that the overlap region between the two beams is isotropic, with a Gaussian profile:

$$\delta V(\mathbf{r}, t) = \frac{V}{\sqrt{2\pi}\sigma} e^{-r^2/2\sigma^2} \cos(\mathbf{q}\cdot\mathbf{r} - \omega t). \tag{33}$$

Here, σ is the width of the Bragg beams and $\mathbf{q}$ and ω are the wavevector and frequency difference between the two beams.

For a Bragg pulse of short duration ($\tau \ll 2\pi/\omega_0$, where ω_0 is the trap frequency), the

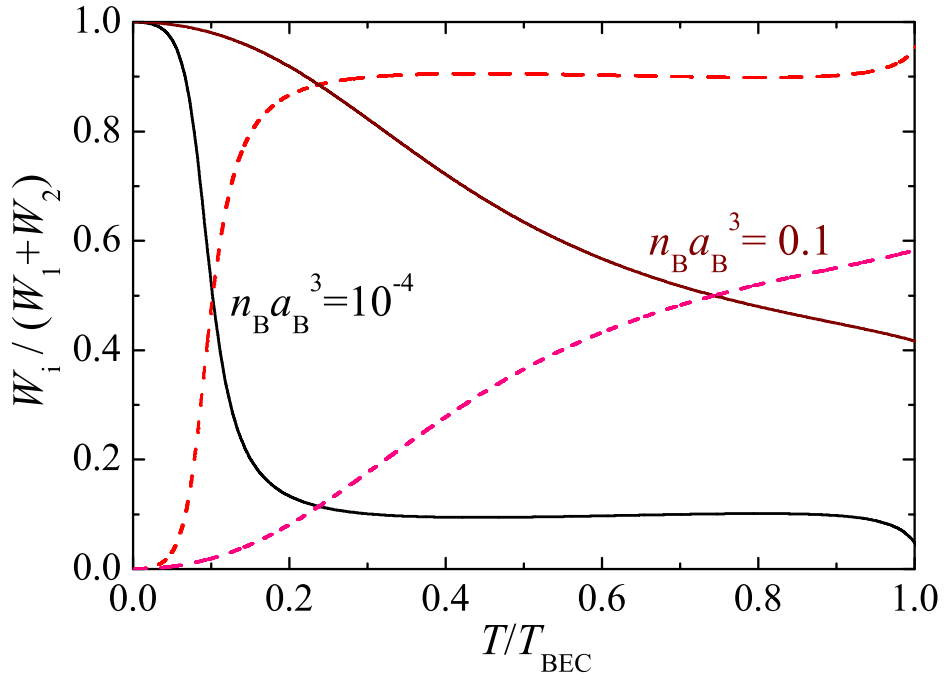

FIG. 8: Temperature dependence of the normalized amplitudes $W_1/(W_1+W_2)$ (solid lines) and $W_2/(W_1+W_2)$ (dashed lines) for a weakly interacting Bose gas ($n_B a_B^3 = 10^{-4}$) and a strongly interacting Bose gas ($n_B a_B^3 = 0.1$).

momentum transferred to the gas is related to the imaginary part of the density response function [see (4)], through a convolution of the atomic density:

$$\Delta P(q,\omega) = \frac{qV^2\tau}{4\pi N\sigma^2}\int d^3r\; n(r) e^{-r^2/\sigma^2} \mathrm{Im}\chi_{nn}(q,\omega;r) \tag{34}$$

In this expression, $\mathrm{Im}\chi_{nn}(q,\omega;r)$ is the imaginary part of the density response function, evaluated within a local density approximation (LDA). The imaginary part of the two-fluid density response function is given by (17) and should be evaluated at the local value of the density. The LDA is justified for wave vectors much larger than the inverse of the size of the trapped gas, so that the system can be considered, locally, as a uniform body.

Results for the momentum transferred given by (34), as a function of ω/qv_F, are shown in figure 9 for $T = 0.75T_c$ and choosing $\sigma = 0.5R_{TF}$, where $R_{TF} \equiv \sqrt{\hbar/m\omega}(24N)^{1/6}$ is the Thomas–Fermi radius of a noninteracting two-component Fermi gas. Although small, the second sound peak is well separated from the first sound peak, revealing that two-photon Bragg spectroscopy might become a practical way to measure second sound. Above and below this temperature, the contribution of second sound to the momentum transfer

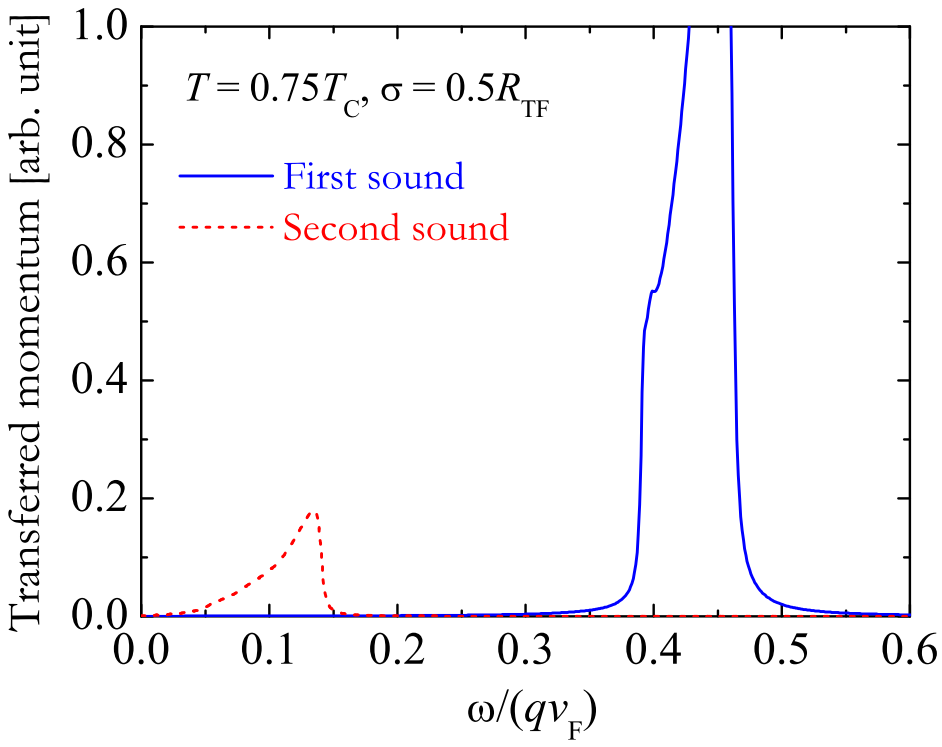

FIG. 9: Momentum transferred to a trapped Fermi gas at unitarity by two photon Bragg scattering due to first and second sound at $T \simeq 0.75T_c$. Solid (blue) line shows the momentum transferred due to first sound as a function of the beam detuning ω divided by the relative wave vector $q \equiv |\mathbf{q}_1 - \mathbf{q}_2|$. v_F is the Fermi velocity. Dashed (red) line shows the momentum transferred due to second sound.

becomes significantly smaller, however.

VII. CONCLUSIONS

In this paper, we have given a detailed analysis of the density response function $\chi_{nn}(q,\omega)$ and the related dynamic structure factor $S(q,\omega)$ for uniform superfluids in the two-fluid hydrodynamic limit. We have put special emphasis on the second sound contribution to $S(q,\omega)$ in the case of a strongly interacting Fermi gas superfluid (at unitarity). While many features of the dynamic structure factor we discuss are known in the superfluid ^{4}He literature [13, 14], several new aspects arise in the case of ultracold superfluid gases.

First and second sound both appear as resonances in the density response function but their relative weights vary in different experimental probes. Two-photon Bragg scattering, a

well-developed tool in ultracold gases used to study density fluctuations (so far, mainly in the collisionless region [20, 38, 39]), is directly proportional to $\mathrm{Im}\chi_{nn}(q,\omega)$. In contrast, the low-frequency limit of the dynamic structure factor $S(q,\omega) = -\mathrm{Im}\chi_{nn}(q,\omega)/\pi n[1-\exp(-\beta\omega)]$ measured in Brillouin light scattering, and also the amplitude of density pulses that can be generated in dilute gases [10], are proportional to $\mathrm{Im}\chi_{nn}(q,\omega)/\omega$. This extra factor of $1/\omega$ leads to a large enhancement of the weight of low frequency second sound in $S(q,\omega)$ compared to first sound.

The relative spectral weights of first and second sound in $\chi_{nn}(q,\omega)$ are very dependent on how strongly temperature fluctuations couple to density fluctuations. For $S(q,\omega)$, this coupling is conveniently parametrized by the value of the dimensionless Landau–Placzek ratio $\epsilon_{\mathrm{LP}} = \gamma - 1$, where γ, defined in (16), is the ratio of the specific heats (per units mass) at constant pressure and volume. At finite temperatures, the relative weight of first and second sound (W_2/W_1) is equal to ϵ_{LP} in both unitary Fermi gases and superfluid ^{4}He. The key difference between superfluid ^{4}He and a unitary Fermi superfluid lies in the value of ϵ_{LP}. Apart from a small region very close to the transition temperature T_c, one has $\epsilon_{\mathrm{LP}} \ll 1$ in superfluid ^{4}He [16, 17]. In contrast, for $T \gtrsim 0.7T_c$, one finds that ϵ_{LP} is of order unity in Fermi superfluids (see figures 3 and 4) and hence the second sound resonance has appreciable weight in $S(q,\omega)$.

Density pulse experiments as suggested in [10] seem to be a promising way of detecting both first and second sound pulses in Fermi gases, although more work is needed to clarify the nature of first and second sound in cylindrical geometries where such pulses would be generated. (See, for instance, recent work on this problem in [40].) The experimental results reported in [22], where a blue-detuned laser was used to generate a density pulse in a Fermi gas close to unitarity, revealed no clear signs of a second sound pulse. This experiment was carried out at very low temperatures, however, where second sound will not have appreciable weight in $S(q,\omega)$ (see figures 3 and 4). Alternately, even though the weight of second sound is comparatively small in Bragg scattering, Bragg scattering has the advantage that it can be used to probe in a very precise way the properties of uniform superfluid Fermi gases [37], including the velocity of second sound.

In section V, we compare the two-fluid hydrodynamics in a uniform, dilute, weakly interacting Bose condensed gas (figure 6) with a strongly interacting Fermi superfluid gas. In such Bose superfluids, the thermal expansion (and hence, ϵ_{LP}) is much larger, with the

result that second sound is the dominant excitation in $S(q,\omega)$ and mainly involves a pure oscillation of the condensate in the presence of a static thermal component [3, 4]. However, first and second sound in a strongly interacting Bose gas are similar to those in a Fermi gas near unitarity (see figure 7).

Acknowledgments

We thank Lev Pitaevskii for useful comments. E.T. was supported by NSF-DMR 0907366 and ARO W911NF-08-1-0338. H.H. and X.-J.L. were supported by ARC and NSFC. S.S. acknowledges the support of the EuroQUAM FerMix program. A.G. was supported by NSERC and CIFAR.

Appendix A: Phonon thermodynamics at low temperatures

At low temperatures, Goldstone phonons determine the thermodynamics of both superfluid ^{4}He and Fermi gases. For phonons with velocity c, the free energy F and normal fluid density ρ_{n0} are given by [41] (Recall that we have set $\hbar = k_B = 1$)

$$F = F_0 - \frac{V\pi^2 T^4}{90c^3} \tag{A1}$$

and

$$\rho_{n0} = \frac{2\pi^2 T^4}{45c^5}. \tag{A2}$$

Using (A1), it is straightforward to show that

$$\bar{s}_0 = -\frac{1}{mN}\left(\frac{\partial F}{\partial T}\right)_{V,N} = \frac{2\pi^2 T^3}{45\rho c^3}, \tag{A3}$$

$$P = -\left(\frac{\partial F}{\partial V}\right)_{T,N} = P_0 + \frac{\pi^2 T^4}{90c^3}\left[1 + \frac{3\rho}{c}\left(\frac{\partial c}{\partial \rho}\right)_{T,N}\right], \tag{A4}$$

and

$$\bar{c}_v = \frac{2\pi^2 T^3}{15\rho c^3}. \tag{A5}$$

In arriving at these expressions, the temperature dependence of the Goldstone phonon velocity c has been ignored. P_0 is the pressure in the ground state. These results can be combined to give

$$\bar{c}_p = \bar{c}_v - T\left(\frac{\partial \bar{s}}{\partial \rho}\right)_T \left(\frac{\partial P}{\partial T}\right)_\rho \left(\frac{\partial P}{\partial \rho}\right)_T^{-1} = \bar{c}_v + \frac{4\pi^4 T^7}{45^2 \rho^2 c^6 v_T^2}\left[1 + \frac{3\rho}{c}\left(\frac{\partial c}{\partial \rho}\right)_T\right]^2, \tag{A6}$$

and

$$v^2 \equiv \bar{s}_0^2 \frac{T}{\bar{c}_v} \frac{\rho_{s0}}{\rho_{n0}} = \frac{c^2}{3} \frac{\rho_{s0}}{\rho_0}. \tag{A7}$$

Combining the above results, the Landau–Placzek ratio at low temperatures is given by

$$\epsilon_{\rm LP} = \frac{2\pi^2 T^4}{135 \rho c^3 v_T^2} \left[1 + \frac{3\rho}{c} \left(\frac{\partial c}{\partial \rho} \right)_T \right]^2 \tag{A8}$$

and hence, recalling that $x = v^2/\gamma v_{\bar{s}}^2$ and $\gamma = v_{\bar{s}}^2/v_T^2$,

$$\sqrt{\frac{\rho_{s0}}{\rho_{n0}} \epsilon_{\rm LP} x} = \frac{1}{3} \frac{\rho_{s0}}{\rho_0} \frac{c^2}{v_{\bar{s}}^2} \left[1 + \frac{3\rho}{c} \left(\frac{\partial c}{\partial \rho} \right)_T \right]. \tag{A9}$$

This result is valid for both the superfluid unitary Fermi gas and superfluid ^{4}He. Further simplifications are not possible without *ab-initio* or experimental information about c. At low temperatures, however, where $\rho_{s0} \simeq \rho_0$ and $v_{\bar{s}} \simeq c$ (see figure 1), (A9) reduces to

$$\sqrt{\frac{\rho_{s0}}{\rho_{n0}} \epsilon_{\rm LP} x} \simeq \frac{1}{3} \left[1 + \frac{3\rho}{c} \left(\frac{\partial c}{\partial \rho} \right)_T \right]. \tag{A10}$$

Equations (A6) and (A7) also give us the result that $\gamma \to 1$ and $x = v^2/\gamma v_{\bar{s}}^2 \to 1/3$ as $T \to 0$. Finally, for a Fermi gas at unitarity, $(\rho/c)(\partial c/\partial \rho)_T = 1/3$ and (A10) is further reduced to the result given in (B10). In superfluid ^{4}He, the Grüneisen constant is almost a factor of 9 larger, $(\rho/c)(\partial c/\partial \rho)_T \simeq 2.84$ [42].

Appendix B: Superfluid and normal fluid velocity fields in second sound

As Landau [2] originally noted, when the thermal expansion coefficient can be neglected (i.e., $\epsilon_{\rm LP} = 0$), one can show that second sound is a pure temperature oscillation, with no associated density fluctuations. This last feature follows from the fact that when $\epsilon_{\rm LP} = 0$, second sound involves no mass current ($\mathbf{j} \equiv \rho_{n0}\mathbf{v}_n + \rho_{s0}\mathbf{v}_s = 0$) and thus the continuity equation requires that $\delta\rho = 0$. Likewise, first sound is a pure density oscillation, and involves no fluctuations in the entropy per unit mass $\bar{s}$. The non-dissipative two-fluid equations give the following equation for this quantity:

$$\frac{\partial \delta \bar{s}}{\partial t} = \frac{\bar{s}_0 \rho_{s0}}{\rho_0} \boldsymbol{\nabla} \cdot (\mathbf{v}_s - \mathbf{v}_n). \tag{B1}$$

This shows that for pure adiabatic motion ($\delta\bar{s} = \delta T = 0$) such as first sound, the superfluid and normal fluid velocities are identical: $\mathbf{v}_s = \mathbf{v}_n$. Putting these results together, the velocity

fields for first and second sound when $\epsilon_{\rm LP} = 0$ are given by

$$\frac{v_s^{(1)}}{v_n^{(1)}} = 1, \quad \frac{\rho_{s0} v_s^{(2)}}{\rho_{n0} v_n^{(2)}} = -1, \tag{B2}$$

where, for instance, $v_s^{(1)}$ denotes the superfluid velocity field associated with first sound (along the direction of propagation $\mathbf{q}$). This Appendix discusses how these velocity ratios change when $\epsilon_{\rm LP}$ is non-zero. Surprisingly, we find that changes are quite substantial at all temperatures, including the low-T region where $\epsilon_{\rm LP} \ll 1$.

As we discuss in the present paper and in [8], the Landau–Placzek ratio $\epsilon_{\rm LP}$ increases with temperature and in Fermi gases near unitarity, $\epsilon_{\rm LP}$ is of order unity at high temperatures (see figure 3). As we have shown, this is large enough that second sound has significant weight in the dynamic structure factor.

To understand the effect that a non-zero value of $\epsilon_{\rm LP}$ has on the superfluid $\mathbf{v}_s$ and normal fluid $\mathbf{v}_n$ velocity fields, one can solve the two-fluid equations for the values of these fields associated with first and second sound $\omega = uq$, where $u = u_1$ or u_2. Defining the variables $\mathbf{j} = \rho_{s0}\mathbf{v}_s + \rho_{n0}\mathbf{v}_n$ and $\mathbf{w} = \rho_{s0}(\mathbf{v}_s - \mathbf{v}_n)$, the plane-wave solutions of the linearized two-fluid equations are

$$\begin{pmatrix} u^2 - v^2 & -s_0 \frac{\rho_{s0}}{\rho_{n0}} \left.\frac{\partial T}{\partial \rho}\right|_{\bar{s}} \\ s_0 \left.\frac{\partial T}{\partial \rho}\right|_{\bar{s}} & u^2 - v_{\bar{s}}^2 \end{pmatrix} \begin{pmatrix} \mathbf{w} \\ \mathbf{j} \end{pmatrix} = 0. \tag{B3}$$

Here,

$$s_0 \left.\frac{\partial T}{\partial \rho}\right|_{\bar{s}} = \frac{\bar{s}_0}{\rho_0} \left.\frac{\partial P}{\partial \bar{s}}\right|_{\rho} = \sqrt{\frac{\rho_{n0}}{\rho_{s0}}} \sqrt{\epsilon_{\rm LP} x} v_{\bar{s}}^2 \equiv b^2 \tag{B4}$$

has units of velocity squared. Recall that x is defined below (24). Standard thermodynamic identities have been used to introduce $\epsilon_{\rm LP} = \gamma - 1$. As the structure of (B3) makes clear, b^2 determines the coupling between density ($\propto \mathbf{j}$) and entropy per unit mass ($\propto \mathbf{w}$) fluctuations. [The latter is given by (B1).]

Using (B3), it is straightforward to derive an expression for the ratio of the velocity fields associated with first and second sound:

$$\frac{v_s}{v_n} = \frac{s_0 \left.\frac{\partial T}{\partial \rho}\right|_{\bar{s}} - \frac{\rho_{n0}}{\rho_{s0}}(u^2 - v_{\bar{s}}^2)}{s_0 \left.\frac{\partial T}{\partial \rho}\right|_{\bar{s}} + (u^2 - v_{\bar{s}}^2)}. \tag{B5}$$

Substituting the expressions for the speeds of first and second sound given by (24) into (B5), one finds

$$\frac{v_s^{(1)}}{v_n^{(1)}} \simeq \frac{v_{\bar{s}}^2 - b^2}{v_{\bar{s}}^2 + \frac{\rho_{s0}}{\rho_{n0}} b^2} \tag{B6}$$

and

$$\frac{\rho_{s0}v_s^{(2)}}{\rho_{n0}v_n^{(2)}} \simeq -\frac{v_{\bar{s}}^2(1-x)+\frac{\rho_{s0}}{\rho_{n0}}b^2}{v_{\bar{s}}^2(1-x)-b^2}. \tag{B7}$$

In section IV, we showed that c_1 and c_2 in (25), which are expansions in the small parameter $\epsilon_{\rm LP}x$, are excellent approximations to the speeds of first and second sound at *all* temperatures (see figure 1). We thus expect (B6) and (B7) to be similarly good approximations for the velocity fields at all temperatures. Using (B4) to remove the dependence of these expressions on $v_{\bar{s}}$, they reduce to

$$\frac{v_s^{(1)}}{v_n^{(1)}} \simeq \frac{1-\sqrt{\frac{\rho_{n0}}{\rho_{s0}}\epsilon_{\rm LP}x}}{1+\sqrt{\frac{\rho_{s0}}{\rho_{n0}}\epsilon_{\rm LP}x}} \tag{B8}$$

and

$$\frac{\rho_{s0}v_s^{(2)}}{\rho_{n0}v_n^{(2)}} \simeq -\frac{(1-x)+\sqrt{\frac{\rho_{s0}}{\rho_{n0}}\epsilon_{\rm LP}x}}{(1-x)-\sqrt{\frac{\rho_{n0}}{\rho_{s0}}\epsilon_{\rm LP}x}}. \tag{B9}$$

When $\epsilon_{\rm LP}$ is set to zero, we recover the results in (B2), describing pure in-phase and out-of-phase oscillations of the superfluid and normal fluid components. However, we note that even though $\epsilon_{\rm LP}$ vanishes as $T \to 0$, so does the normal fluid density ρ_{n0}, and it is not obvious that $\sqrt{\rho_{s0}\epsilon_{\rm LP}x/\rho_{n0}}$ is small at low temperatures. Conversely, at high temperatures, $T \to T_c$, the factor of $\sqrt{\rho_{n0}/\rho_{s0}}$ multiplying $\sqrt{\epsilon_{\rm LP}x}$ in (B8) and (B9) will enhance the small parameter $\sqrt{\epsilon_{\rm LP}x}$. It is thus crucial to know the temperature dependencies of ρ_{s0}/ρ_{n0} and $\epsilon_{\rm LP}x$ in both limits.

At low temperatures, the thermodynamics is dominated by Goldstone phonons. Using standard results in the phonon regime, one can show (see A) that in the $T \to 0$ limit,

$$\sqrt{\frac{\rho_{s0}}{\rho_{n0}}\epsilon_{\rm LP}x} \simeq \frac{2}{3} \tag{B10}$$

for a unitary Fermi gas. This non-zero limiting value as $T \to 0$ arises from the fact that *both* $\epsilon_{\rm LP}x$ and ρ_{n0} vanish as T^4. For a Fermi gas at unitarity in the $T \to 0$ limit, using (B10) and the fact that $x = 1/3$ (see A), (B8) and (B9) give

$$\frac{v_s^{(1)}}{v_n^{(1)}} \simeq \frac{3}{5}, \quad \frac{\rho_{s0}v_s^{(2)}}{\rho_{n0}v_n^{(2)}} \simeq -2, \tag{B11}$$

even though $\epsilon_{\rm LP}$ vanishes as $T \to 0$ (as shown in figure 3). If we had simply set $\epsilon_{\rm LP} = 0$, as often done in the superfluid literature, we would instead obtain the results given by (B2).

In figure 10, we plot the velocity ratios in (B8) and (B9) for a superfluid unitary Fermi gas. It is clear that the superfluid and normal fluid velocities which are involved in first

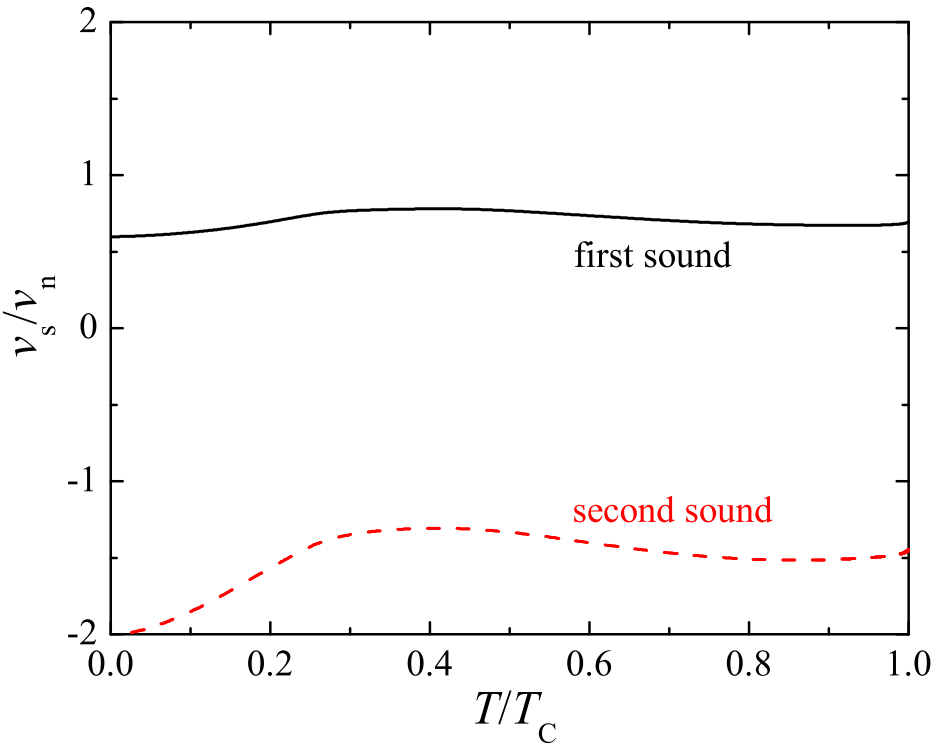

FIG. 10: Superfluid and normal fluid velocity fields associated with first and second sound in a unitary Fermi superfluid. The solid (black) line shows the ratio $v_s^{(1)}/v_n^{(2)}$ of the superfluid and normal fluid velocity fields involved with first sound, (B8). The dashed (red) line shows the ratio $\rho_{s0}v_s^{(2)}/\rho_{n0}v_n^{(2)}$ of the superfluid and normal fluid currents associated with second sound, (B9). If we set $\epsilon_{\rm LP} = 0$, these ratios would be 1 and -1, respectively, describing the velocity fields for pure density and temperature oscillations.

and second sound are significantly different from those given in (B2). This is a reflection of the fact that first and second sound are not pure uncoupled density and temperature waves, respectively, which would be described by (B2) and correspond to $\epsilon_{\rm LP} = 0$ (and $\rho_{n0} \neq 0$). As we have shown in [8], such in-phase ($\mathbf{v}_s = \mathbf{v}_n$) and out-of-phase zero current ($\mathbf{j} = 0$) solutions correspond to first and second sound velocities given by

$$u_1^2 = v_{\bar{s}}^2, \quad u_2^2 = T\frac{\bar{s}_0^2}{\bar{c}_v}\frac{\rho_{s0}}{\rho_{n0}} \equiv v^2. \tag{B12}$$

As we show in figure 2 of [8], these sound velocities are in good agreement with a full calculation including the coupling associated with $\epsilon_{\rm LP}$. In this Appendix and section IV, we have carried out a careful analysis based on expanding to first order in the parameter $\epsilon_{\rm LP}x$, which is small ($\ll 1$) at all temperatures [14, 15]. The results in figure 10 show that the

main effect of working with γ not equal to unity is simply that the second sound speed u_2 is given by $v/\sqrt{\gamma}$ as in (25), instead of v in (B12). In contrast, the first sound speed is always very well approximated by $v_{\bar{s}}$, even when γ deviates from unity.

Initially, it seems surprising that the superfluid and normal fluid velocity fields shown in figure 10 are so different from those in (B2), since the first and second sound velocities are fairly well approximated by (B12). (See figure 2 of [8].) This arises because of two features evident in (B8) and (B9). First of all, we note that the first and second sound speeds in (24) involve corrections of order $\epsilon_{\rm LP} x \ll 1$, while the related corrections are much larger in (B9) and (B11) since they enter as $\sqrt{\epsilon_{\rm LP} x}$. The second, and more important, reason is that the corrections involve the factors $\sqrt{\rho_{s0}/\rho_{n0}}$ and $\sqrt{\rho_{n0}/\rho_{s0}}$, which are very large at $T = 0$ and $T = T_c$, respectively.

Substantial deviations from the ratios given in (B2) also occur in superfluid ^{4}He, although the magnitude will be different from the case of a Fermi superfluid at unitarity shown in figure 10. This feature was not commented on in the older superfluid ^{4}He literature [14, 15, 31], which concentrated entirely on the frequency and damping of the first and second sound resonances appearing in the dynamic structure factor. The associated velocity fields calculated here were not discussed. These velocity fields may be direct experimental interest in future studies of two-fluid hydrodynamics in Fermi superfluids.

Calculation shows that the various terms in (B8) and (B9) are not small compared to unity. However, if one formally expands these expressions to leading order in $b^2/v_{\bar{s}}^2$ ($= \sqrt{\rho_{n0}\epsilon_{\rm LP} x/\rho_{s0}}$), one finds

$$\frac{v_s^{(1)}}{v_n^{(1)}} = 1 - \delta, \quad \frac{\rho_{s0} v_s^{(2)}}{\rho_{n0} v_n^{(2)}} = -1 - \delta, \tag{B13}$$

where the leading correction to (B2) is found to be

$$\delta = \frac{\rho_0}{\rho_{n0}} \frac{b^2}{v_{\bar{s}}^2} = \frac{\rho_0}{\rho_{n0}} \sqrt{\frac{\rho_{n0}}{\rho_{s0}} \epsilon_{\rm LP} x}. \tag{B14}$$

This value of δ agrees with the expression originally worked out by Lifshitz (see page 71 in [43]) in the limit where $u_2^2 \ll u_1^2$, valid close to T_c. In the case of superfluid ^{4}He, the fact that $\epsilon_{\rm LP} \ll 1$ even close to T_c (it diverges very weakly at T_c) means that the first correction in (B13) is indeed small, $\delta \ll 1$. In contrast, for a Fermi gas at unitarity, $\epsilon_{\rm LP}$ is of order unity or larger near T_c (see figure 3) and as a result we find $\delta = 0.3$ just below T_c [44]. In

this case, the expansion in (B13) is not valid, as can be seen by comparing (B13) with the results in figure 10.

---

[1] For a review, see J. Wilks, *The properties of liquid and solid Helium*, (Clarendon Press, Oxford, 1967).

[2] L. D. Landau, J. Phys. (U.S.S.R.) **5**, 71 (1941).

[3] A. Griffin, T. Nikuni and E. Zaremba, *Bose-condensed gases at finite temperatures*, (Cambridge, N.Y., 2009).

[4] R. Meppelink, S. B. Koller, and P. van der Straten, Phys. Rev. A **80**, 043605 (2009).

[5] For a review of strongly interacting Fermi gases see S. Giorgini, L. P. Pitaevskii, and S. Stringari, Rev. Mod. Phys. **80**, 1215 (2008).

[6] E. Taylor and A. Griffin, Phys. Rev. A **72**, 053630 (2005).

[7] E. Taylor, H. Hu, X-J. Liu, and A. Griffin, Phys. Rev. A **77**, 033608 (2008).

[8] E. Taylor, H. Hu, X.-J. Liu, L. P. Pitaevskii, A. Griffin, and S. Stringari, Phys. Rev. A **80**, 053601 (2009).

[9] E. Zaremba, T. Nikuni, and A. Griffin, Journ. Low Temp. Phys. **116**, 277 (1999).

[10] E. Arahata and T. Nikuni, Phys. Rev A **80**, 043613 (2009).

[11] P. C. Hohenberg and P. C. Martin, Phys. Rev. Lett. **12**, 69 (1964).

[12] P. C. Hohenberg and P. C. Martin, Ann. Phys. (N.Y.) **34**, 291 (1965).

[13] See, for example, T. J. Greytak in *Low Temperature Physics LT13*, ed. by K. D. Timmermans, W. J. O'Sullivan, and E. F. Hammel (Plenum Press, N.Y. 1974), page 9.

[14] W. F. Vinen in *Physics of Quantum Fluids*, ed. by R. Kubo and F. Takano (Syokabo Publishing Company, Tokyo, 1970), page 1.

[15] P. C. Hohenberg, *Journ. Low Temp. Phys.* **11**, 745 (1973).

[16] G. Winterling, F. S. Holmes, and T. J. Greytak, Phys. Rev. Lett. **30**, 210 (1973).

[17] J. T. O'Connor, C. J. Palin, and W. F. Vinen, J. Phys. C: Solid State Phys. **8**, 101 (1975).

[18] L. P. Pitaevskii and S. Stringari, *Bose-Einstein condensation* (Oxford University Press, Oxford, 2003).

[19] A. Griffin, *Excitations in a Bose-condensed liquid*, (Cambridge, N.Y. 1993), chapter 2.

[20] D. M. Stamper-Kurn, A. P. Chikkatur, A. Görlitz, S. Inouye, S. Gupta, D. E. Pritchard, and

W. Ketterle, Phys. Rev. Lett **83**, 2876 (1999).

[21] M. R. Andrews, D. M. Kurn, H.-J. Miesner, D. S. Durfee, C. G. Townsend, S. Inouye, and W. Ketterle, Phys. Rev. Lett. **79**, 553 (1997).

[22] J. Joseph, B. Clancy, L. Luo, J. Kinast, A. Turlapov, and J. E. Thomas, Phys. Rev. Lett. **98**, 170401 (2007).

[23] P. Nozières and D. Pines, *Theory of quantum liquids, Vol. II: Superfluid Bose liquids*, (Addison-Wesley, Redwood city, California, 1990).

[24] See, for example, G. F. Mazenko, *Nonequilibrium statistical mechanics*, (Wiley - VCH, N.Y., 2006), chapter 6.

[25] P. Nozières and S. Schmitt-Rink, J. Low Temp. Phys. **59**, 195 (1985).

[26] H. Hu, X.-J. Liu, and P. D. Drummond, Phys. Rev. A **73**, 023617 (2006).

[27] The superfluid density scales as $\rho_{s0} \propto (T-T_c)^{2/3}$ close to T_c, as first shown by B. D. Josephson, Phys. Lett. **21**, 608 (1966). For details on how we fit our NSR data to this asymptotic behaviour close to T_c, see [7].

[28] N. Fukushima, Y. Ohashi, E. Taylor, and A. Griffin, Phys. Rev. A **75**, 033609 (2007).

[29] E. Taylor, Phys. Rev. A **80**, 023612 (2009).

[30] W. F. Vinen, J. Phys. C: Solid State Phys. **4**, L287 (1971).

[31] R. A. Ferrell, N. M. Menyhard, H. Schmidt, F. S. Schwabl, and P. Széfpalusy, Ann. Phys. (N.Y.) **47**, 565 (1968).

[32] L. D. Landau and G. Placzek, Phys. Z. Soviet Union, **5**, 172 (1934).

[33] D. S. Petrov, C. Salomon, and G. V. Shlyapnikov, Phys. Rev. Lett. **93**, 090404 (2004).

[34] H. Shi and A. Griffin, Phys. Rep. **304**, 1 (1998).

[35] Y. He, C.-C. Chien, Q. Chen, and K. Levin, Phys. Rev. B **76**, 224516 (2007).

[36] Figures 7 and 8 of [10], showing first and second sound in a strongly interacting molecular Bose gas, are incorrect. The corrected results agree with our figures 7 and 8. For details, see erratum, E. Arahata and T. Nikuni, Phys. Rev. A **81**, 029904 (2010).

[37] D. E. Miller, J. K. Chin, C. A. Stan, Y. Liu, W. Setiawan, C. Sanner, and W. Ketterle, Phys. Rev. Lett. **99**, 070402 (2007).

[38] N. Katz, R. Ozeri, J. Steinhauer, N. Davidson, C. Tozzo, and F. Dalfovo, Phys. Rev. Lett. **93**, 220403 (2004).

[39] R. Ozeri, N. Katz, J. Steinhauer, and N. Davidson, Rev. Mod. Phys. **77**, 187 (2005).

[40] G. Bertaina, L. Pitaevskii, and S. Stringari, arXiv:1002.0195.

[41] E. M. Lifshitz and L. P. Pitaevskii, *Statistical Physics, Part 2* (Butterworth-Heinemann, Oxford, 2002).

[42] B. M. Abraham, Y. Eckstein, J. B. Ketterson, M. Kuchnir, and P. R. Roach, Phys. Rev. A **1**, 250 (1970).

[43] I. M. Khalatnikov, *Introduction to the theory of superfluidity*, (W. A. Benjamin, N.Y., 1965).

[44] With a better theory of the thermodynamics than NSR, we would find that δ diverges at $T = T_c$ (as it does in superfluid ^{4}He). Our point here is that it is also significant in a large region below T_c.